Laser transmission welding of composites-Part A: Thermo-physical and optical characterization of materials

Andre Chateau Akue Asseko, Benoît Cosson, Fabrice Schmidt, Yannick Le Maoult, Eric Lafranche

▶ **To cite this version:**

Andre Chateau Akue Asseko, Benoît Cosson, Fabrice Schmidt, Yannick Le Maoult, Eric Lafranche. Laser transmission welding of composites-Part A: Thermo-physical and optical characterization of materials. Infrared Physics and Technology, 2015, 72, p. 293-299. 10.1016/j.infrared.2015.02.004 . hal-01611009

HAL Id: hal-01611009
https://hal.science/hal-01611009

Submitted on 15 Feb 2019

HAL is a multi-disciplinary open access archive for the deposit and dissemination of scientific research documents, whether they are published or not. The documents may come from teaching and research institutions in France or abroad, or from public or private research centers.

L'archive ouverte pluridisciplinaire **HAL**, est destinée au dépôt et à la diffusion de documents scientifiques de niveau recherche, publiés ou non, émanant des établissements d'enseignement et de recherche français ou étrangers, des laboratoires publics ou privés.

Laser transmission welding of composites-Part A: Thermo-physical and optical characterization of materials

André Chateau Akué Asséko [a,b,c,*], Benoît Cosson [a,c], Fabrice Schmidt [b], Yannick Le Maoult [b], Eric Lafranche [a,c]

[a] Mines Douai, Department of Polymers and Composites Technology & Mechanical Engineering, 941 rue Charles Bourseul, CS 10838, F-59508 Douai Cedex, France
[b] Université de Toulouse, Mines Albi, ICA (Institut Clément Ader), Campus Jarlard, F-81013 Albi cedex 09, France
[c] Université de Lille Nord de France, 59000 Lille, France

A B S T R A C T

In the present study, thermophysical and optical characterization of UD thermoplastic composites materials have been investigated. Knowledge of these parameters is of utmost importance to better understanding of any process that involves laser processing of materials. These properties play an important role during the simulation of the welding process. Two optical parameters namely transmission factor (T_λ) and reflection factor (R_λ) are measured using IRFT spectrometer and integrating sphere at the laser wavelength. The transmittivity coefficient (τ_λ) and reflectivity coefficient (ρ_λ) were determined using two approaches. A simplified experimental approach and numerical approach based on an inverse method program. Comparison between the two approaches is presented. A well-design device has been also developed in order to evaluate anisotropic thermal conductivities of composites. And finally we compared the experimental results to the analytical method concerning modeling thermal conductivities in composites.

Keywords:
Laser welding
Optical properties
Thermal properties
Thermoplastics composites
Experimental setup
Inverse method

Contents

* Corresponding author at: Mines Douai, Department of Polymers and Composites Technology & Mechanical Engineering, 941 rue Charles Bourseul, CS 10838, F-59508 Douai Cedex, France.

E-mail addresses: andre.akue.asseko@mines-douai.fr (A.C.A. Asséko), cosson@mines-douai.fr (B. Cosson), fabrice.schmidt@mines-albi.fr (F. Schmidt), yannick.lemaoult@mines-albi.fr (Y.L. Maoult), eric.lafranche@mines-douai.fr (E. Lafranche).

Nomenclature

x, y, z	space variables	r_λ	reflectivity coefficient
σ_x	scattering standard deviation (m)	τ_λ	transmittivity coefficient
D	optical scattering coefficient (m^{-1})	k	thermal conductivity tensor (W/m K)
K	absorption coefficient (m^{-1})	$Cp(T)$	specific heat (J/kg K)
T_λ	transmission factor	T	temperature (K)
R_λ	reflection factor	r_{spot}	radius of the focused spot (mm)

1. Introduction

In our previous studies [1–3], a global analytical model (refraction and absorption phenomena) for modeling of transmission laser/infrared welding process in thermoplastic composites has been developed. This model allows describing the attenuation of the laser beam, the prediction of the heat source in the laser welding process thermal simulations, in the case of UD thermoplastic composites materials. And finally the model permits to determine the three dimensional temperature fields, during the welding process. In order to compute the temperature field, the optical and thermal properties of the welded materials are necessary as input parameters in order to model the process properly [4–13]. These properties vary depending on the component material (fiber and matrix), their assembly, and the volume fraction in the considered composite [14].

2. Laser/infrared welding process of thermoplastic composites

Transmission laser/infrared welding technique [15] presents specific advantages for industrial applications over other conventional technologies:

- the method is accurate and flexible,
- small heat affected zone, easy to automate and control and non-contaminant,
- heat transfer with the ability to optimize the welding temperature (at the interface of the welding zone),
- absence of vibration during the welding process (contrary to the ultrasonic welding, friction welding),
- fast welding speed for welding plastic parts with an acceptable welding time.

Transmission laser/infrared welding of composites involves two joining parts: one semi-transparent to the IR wavelengths and the other part is absorbent in the same wavelengths. The two parts are positioned together before the welding. Surface treatments are not need as in the gluing process. The laser beam energy is transmitted through the semi-transparent material and is absorbed within the surface of the second materials (Fig. 1). The bonding between the two parts allows the heating of the semi-transparent part by thermal conduction. Thus, melting and fusion of both materials interface occurs (the bonding between the two parts occurs when $T > T_{melt}$ in this area). The energy is deposited at the interface in a localized zone causing the formation of a weld zone. Comparing with welding traditional techniques, laser welding efficiency strongly depends on the optical properties of the material [14]: absorption, transmission, refraction, reflection, scattering and thermal properties: specific heat, thermal conductivities and density.

The semi-transparent material considered in this study is Polycarbonate (PC) Macrolon 2405 with glass fiber 40%. The wavelength used for the measurement is 0.940 μm (diode laser wavelength).

3. Determination of optical properties

3.1. Transmission and reflection factors measurements

The optical characterization enables to describe the interaction between the incident laser beam and the semi-transparent composite. When radiation (e.g. laser source) reaches the surface of a material, a portion may be reflected, another portion may be absorbed or diffused and transmitted. The Fig. 2 sketches the mechanism of light transmission in the semi-transparent composite part. During transmission laser welding process, a divergence of

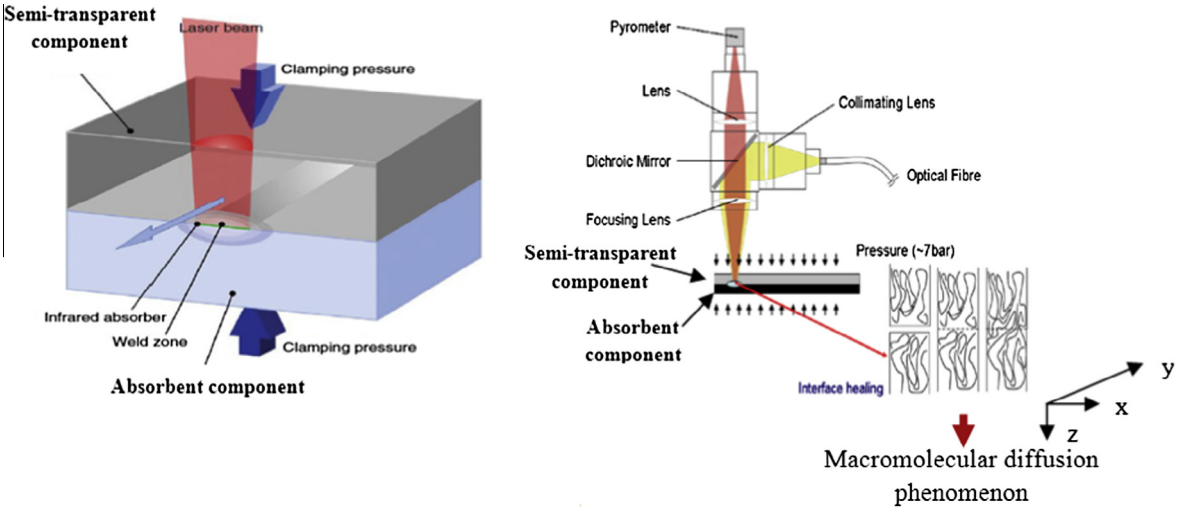

Fig. 1. Laser welding system [15].

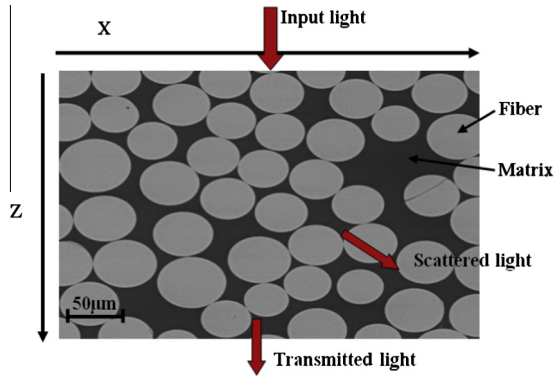

Fig. 2. Light transmission in semi-transparent composite part (microscopic observations of the Polycarbonate (PC) Macrolon 2405 with glass fiber 40%).

the laser beam is observed in the first part due to the internal refraction at the microscopic scale of the beam at each matrix-fiber interface. At the macroscopic scale, this phenomenon leads to the light scattering of the laser beam in this heterogeneous media. The absorption (K_λ) was assumed to be negligible compared to the scattering effect (D_λ) as in [2].

For the determination of the transmittivity (τ_λ) and reflectivity (ρ_λ) coefficients of semi-transparent material, transmission factor (T_λ) and reflection factor (R_λ) are measured using IRFT spectrometer (0.8–25 µm) and integrating sphere at the laser wavelength for different samples as described in Fig. 3 below.

Fig. 4 shows in the near IR (NIR) spectral range ($\Delta\lambda$ = 0.8–2 µm), the transmission and the reflection spectrums factors of the reinforced PC with glass fiber composite versus thickness (d). Fig. 5 illustrates the results of the average spectral diffuse reflection factor measurement via an integrating sphere to the composite surface (sample thickness = 1.64 mm). The value obtained (Eq. (1)) is R = 20% in near infrared spectral range.

$$R(T_0) = \frac{\int_{0.8\mu m}^{2\mu m} R_\lambda L_\lambda^0(T_0)d\lambda}{\int_{0.8\mu m}^{2\mu m} L_\lambda^0(T_0)d\lambda} \tag{1}$$

In the literature [4] there are two expressions which provides transmission factor (T_λ) and reflection factor (R_λ) values depending on the transmittivity (τ_λ) and the reflectivity (ρ_λ) coefficients (Eqs. (2) and (3)).

$$T_\lambda = \frac{(1-\rho\lambda)^2\tau_\lambda}{1-(\rho_\lambda\tau_\lambda)^2} \tag{2}$$

$$R_\lambda = \rho\lambda\left[1+\tau_\lambda^2\frac{(1-\rho_\lambda)^2\tau^2\lambda}{1-(\rho_\lambda\tau_\lambda)^2}\right] \tag{3}$$

The analytical solution for the determination of τ_λ and ρ_λ is difficult. In our case we have considered two approaches to find these material intrinsic parameters: a simplified experimental approach which has already been proven in several studies [16,17] and numerical approach based on an inverse method program.

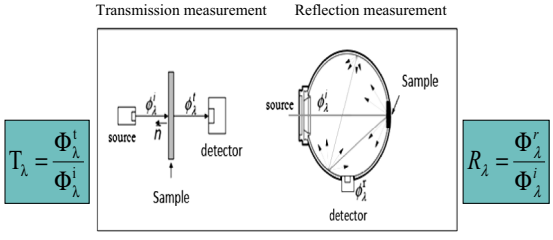

Fig. 3. Light transmission in semi-transparent composite part.

3.2. A simplified experimental approach

This approach assumes that a simplified form of Eq. (2) considering some assumptions. By writing in the first time the Eq. (2) in another form, we obtain (Eq. (5)):

$$T_\lambda = (1+\rho_\lambda)\frac{(1-\rho_\lambda)}{1+\rho_\lambda}\frac{(1-\rho_\lambda)\tau_\lambda}{1-(\rho_\lambda\tau_\lambda)^2} \tag{4}$$

$$T_\lambda = \tau_\lambda\frac{(1-\rho_\lambda)}{1+\rho_\lambda}\frac{1-\rho_\lambda^2}{1-(\rho_\lambda\tau_\lambda)^2} \tag{5}$$

And considering following assumptions [4] such as:

- $\rho_\lambda \ll 1$ For polymers materials
- $(\rho_\lambda\tau_\lambda)^2 \ll 1$

This leads that the following expression $A = \frac{1-\rho_\lambda^2}{1-(\rho_\lambda\tau_\lambda)^2} \approx 1$. Finally, we find a simplified expression of the transmission factor (Eq. (6)).

$$T_\lambda = \approx \tau_\lambda\frac{1-\rho_\lambda}{1+\rho_\lambda} \tag{6}$$

We plotted the evolution of the term $A = \frac{1-\rho_\lambda^2}{1-(\rho_\lambda\tau_\lambda)^2}$ versus wavelength in order to justify this approximation (Fig. 6). It is noted that at the laser wave length (0.940 µm), this expression roughly tends to 1 (0.99) and the average error on the whole spectrum is 5%.

Eq. (6) highlights the relationship between transmittivity and the measurement sample thickness. It comes to study the light scattering in the semi-transparent composite. Based on Eq. (6), we obtain the following expression [16,17]:

$$-\ln T_\lambda = -\ln\tau_\lambda + \ln\frac{1+\rho_\lambda}{1-\rho_\lambda} = D_\lambda \times d + C_\lambda \tag{7}$$

With:

$$\tau_\lambda = e^{-D_\lambda \times d} \tag{8}$$

where according to the Beer-Lambert law τ_λ gives (8) and C_λ is a value corresponding to calculation of the $-\ln(T_\lambda)$ intercept of the experimental line (Fig. 7). This value permits to obtain the reflectivity value. This figure shows the variation of the natural logarithm of the spectral transmission factor versus the sample thickness.

Results on the Fig. 7 give the light scattering coefficient by the calculation of the slope of the experimental line. The light scattering coefficient value obtained is $D_{\lambda=0.940\mu m}$ = 740 m^{-1}.

3.3. A numerical approach

Numerical approach is based on an inverse method program using Eqs. (2) and (3). We identified τ_λ and ρ_λ using a SQP (Sequential Quadratic Programming) estimation algorithm which is an iterative method for nonlinear optimization. The fmincon function in Matlab software permitted to find the τ_λ and ρ_λ parameters with the following equation system (Eq. (9)). We fixed the initial guess value for the τ_o and ρ_o to begin iteration:

$$\begin{cases} T_\lambda = \frac{(1-\rho_\lambda)^2\tau_\lambda}{1-(\rho_\lambda\tau_\lambda)^2} \\ R_\lambda = \rho_\lambda\left[1+\tau_\lambda^2\frac{(1-\rho_\lambda)^2\tau_\lambda^2}{1-(\rho_\lambda\tau_\lambda)^2}\right] \end{cases} \tag{9}$$

The double objective function J used is (Eq. (10)):

$$J = \left|\frac{T_{\text{experimental}} - T_{\text{numerical}}}{T_{\text{experimental}}}\right| + \left|\frac{R_{\text{experimental}} - R_{\text{numerical}}}{R_{\text{experimental}}}\right| \tag{10}$$

where $T_{\text{experimental}}$ and $R_{\text{experimental}}$ were the measured transmission and reflection factors data. $T_{\text{numerical}}$ and $R_{\text{numerical}}$ were the found

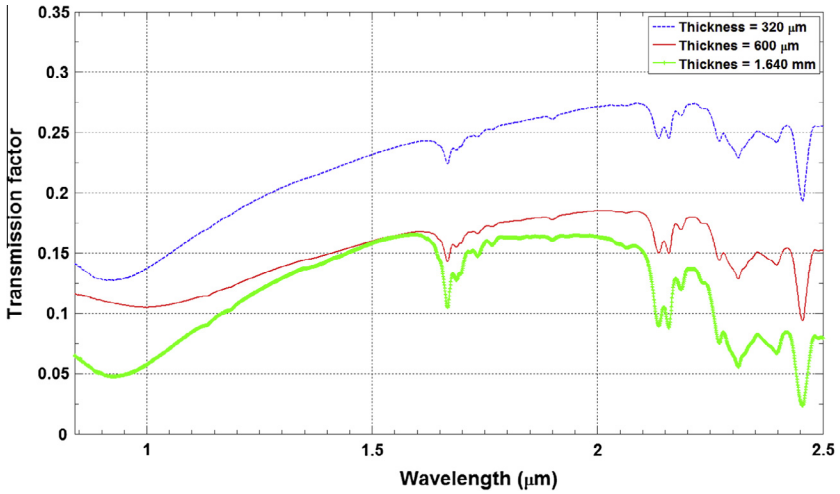

Fig. 4. Transmission factor measurement for PC–glass composite part versus wavelength.

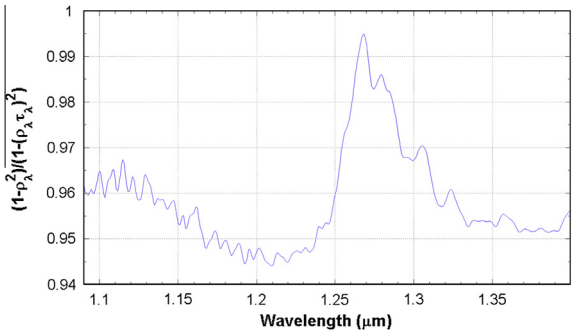

Fig. 5. Spectral diffuse reflection factor measurement using integrating sphere.

transmission and reflection factors data after iteration. Numerical approach results is compared to simplified approach results (Figs. 8 and 9) for the determination of τ_λ and ρ_λ. The comparison shows a fair agreement between them. The error between the two approaches is less 2%.

4. Thermal characterization of reinforced UD Polycarbonate (PC) with glass fiber

Thermal properties of the materials constituting the composite are different; a factor around 4 exists between resin and fibers conductivities for instance [14]. Moreover, the final composite thermal properties also depend on the spatial organization of its constituents, resulting in anisotropic macroscopic effective properties. The thermal conductivity measurement in the composite is not easy; on one hand the material is anisotropic and heterogeneous. In this study, an experimental well-design device has been developed in order to evaluate orthotropic conductivity tensor (k_x, k_y, k_z). A composite sample is submitted on its front face to a heat flux from a halogen lamp MAZDA GY.6.35 (nominal power: 50 W, 12 V) (Fig. 10) focused by an ellipsoidal reflector; thus forming a beam considered as a gaussian shape. The lamp is a polychromatic source. The reflection percentage of reflectors is close to 90% (manufacturer data). The focused lamp enables to simulate a localized heating. The heat flux is concentrated on a small area as a laser.

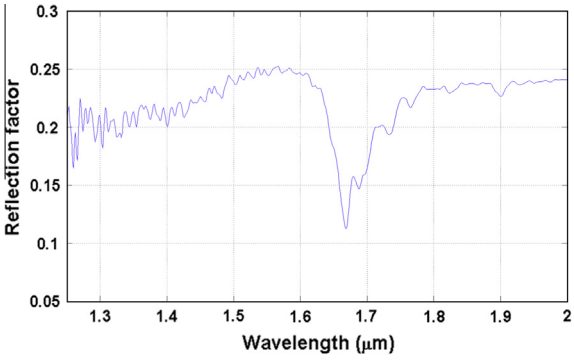

Fig. 6. Variation of A versus wavelength.

The temperature field on the back face is then measured using a CS 325 FLIR infrared camera [7.5–13.5 µm]. The infrared camera has been calibrated between 273.15 K and 973.15 K during the process. From its evolution of temperature, the conductivities of the material according to its anisotropy directions is estimated by inverse method as in [18] using COMSOL Multiphysics software via its optimization toolbox. The optimization solver used is the solver SNOPT [19]. The optimization criterions will use horizontal and/or measured vertical temperature profiles at the back surface of the composite. In this study, a set of points on the plate is defined (Fig. 11).

The objective is to minimize the squared difference between the experimental and simulated temperatures profiles. A least squares criterion F is then defined as follows [20]:

$$F = \sum \int_0^t \left(T_{\text{experimental}}(\text{points}) - T_{\text{simulated}}(\text{points})\right)^2 \qquad (11)$$

The heat diffusion (light scattering) into the semi-transparent composite thickness is related to its transverse thermal conductivity (k_z) and along the perpendicular plane to the thickness of the composite to its longitudinal thermal conductivities (k_x, k_y) which also have an influence on the shape of thermal affected zone. In our study, each reinforcement tissue is made of unidirectional glass fibers assembled in a quasi-isotropic draping as in [21]. The initial parameters for the numerical simulation are referenced in Table 1.

Numerical simulation is compared to experimental data (Fig. 12) versus time. The value of the error at convergence is less than 5%. The agreement between simulations and experiments is fair. The Table 2 shows the results of the global conductivity tensor (k_x, k_y, k_z) of the PC glass fiber composite for several tests.

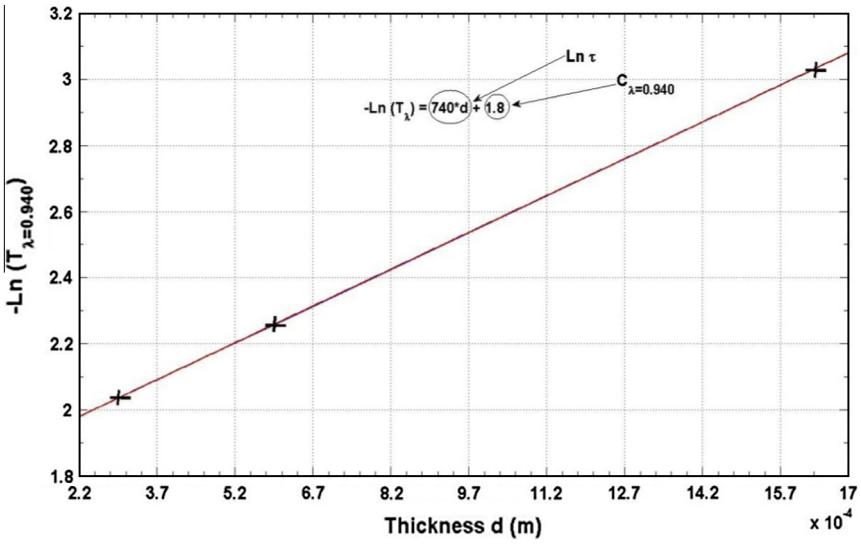

Fig. 7. The variation of the natural logarithm of the spectral transmission factor versus thickness (λ = 0.940 μm).

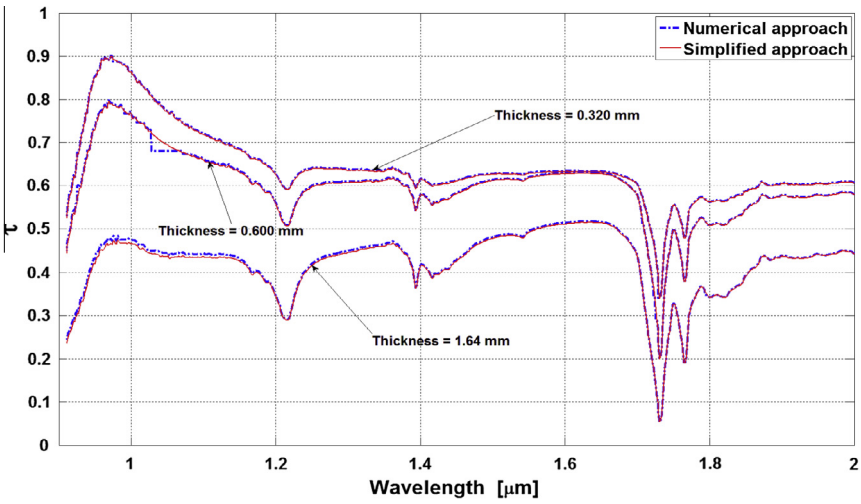

Fig. 8. Transmittivity coefficient for PC–glass composite versus wavelength.

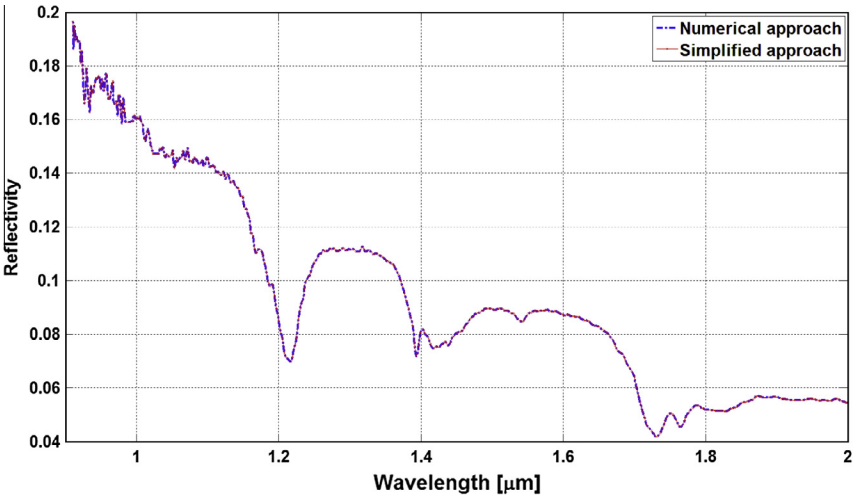

Fig. 9. Reflectivity coefficient for PC–glass composite versus wavelength (d = 1.64 mm).

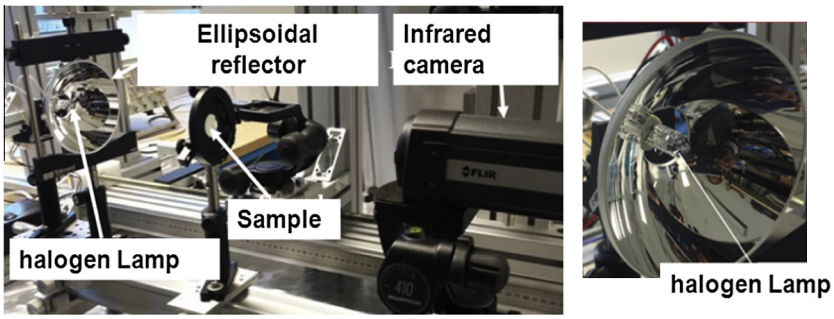

Fig. 10. Experimental set-up.

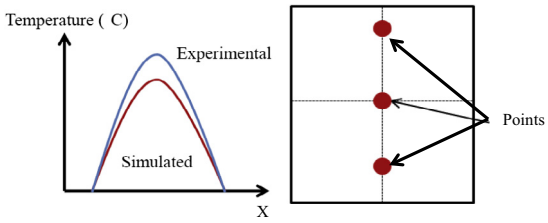

Fig. 11. Optimization criterion.

Table 1
Initial parameters for the numerical simulation.

Properties	Dimensions	PC glass fiber (40%) composite
Thickness	d [mm]	1.64
Length	L [mm]	50
Width	l [mm]	30
Scattering coefficient	D [m^{-1}]	740 [2]
Density	rho [$kg.m^{-3}$]	1519
Initial temperature	T [°C]	20
Radius of the focused spot	r_{spot} [mm]	7
Scattering standard deviation	σ_x [mm] for d = 1.64 mm	21 [2]

As a preliminary validation, we compared our results to the analytical method developed in [20] concerning modeling thermal conductivities in the unidirectional composites. This method used two steps. The first step consists in determining the transverse and longitudinal thermal conductivities of a single unidirectional lamina in which the fibers are parallel. In the second step, the different orientations of fibers in the stacking sequence are considered to obtain the laminate thermal conductivity tensor. The analytical method is based on an isotropic case due to a homogeneous fibers distribution in the x and z plane. This leads to $k_x = k_z$. However the real microstructure of our composite is a quasi-unidirectional and the analytical model is less realistic, which causes a variation of the conductivities in the x and z plane (see Table 3).

Measurements of the specific heat capacity of the materials were carried out by Differential Scanning Calorimetry using a Perkin Elmer calorimeter. Measurements are performed under an inert nitrogen atmosphere between 20 °C and 220 °C (Fig. 13).

The glass transition temperature T_g of the amorphous polymer PC with glass fiber composite is close to 135 °C (PC glass fiber) which leads a change of the specific heat capacity of the material. For the infrared heating simulations in next study, the specific heat capacity will be interpolated in order to obtain a polynomial form that is a function of the temperature.

Table 2
Simulated thermal conductivities.

	k_y (W m^{-1} K^{-1})	k_x (W m^{-1} K^{-1})	k_z (W m^{-1} K^{-1})
Test 1	0.305	1207	0.14
Test 2	0.2987	0.197	0.125
Test 3	0.3107	0.2059	0.152
Average	0.305	0.201	0.139

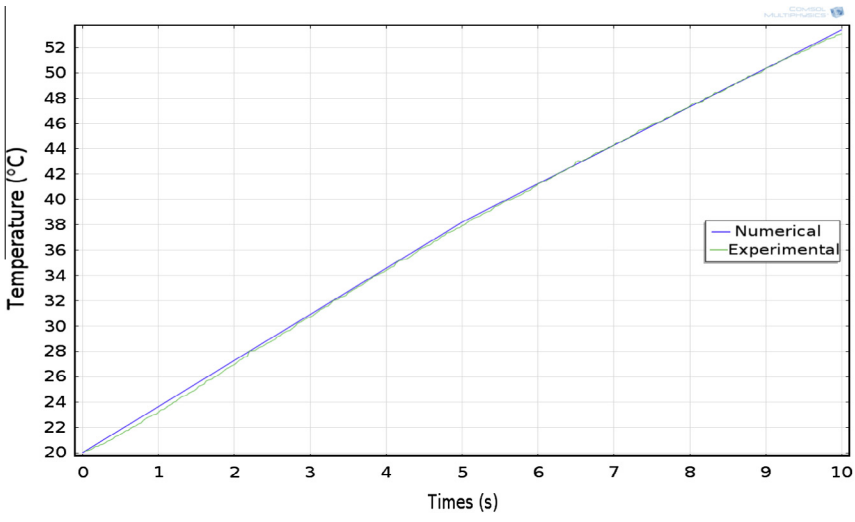

Fig. 12. Experimental and numerical temperatures at the centre of the rear face of the PC glass fiber.

Table 3
Comparison experimental and analytical thermal conductivities.

PC glass fiber (40%) (k_{PC} = 0.2 W m^{-1} K^{-1}) (k_{fiber} = 1 W m^{-1} K^{-1})	Longitudinal thermal conductivities: k_x (W m^{-1} K^{-1}) (transverse direction to the fibers in the plane)	Longitudinal thermal conductivities: k_y (W m^{-1} K^{-1}) (parallel direction to the fibers)	Transverse thermal conductivity k_z (W m^{-1} K^{-1})
Experimental method	0.201	0.305	0.139
Analytical method [20]	0.176	0.28	0.176

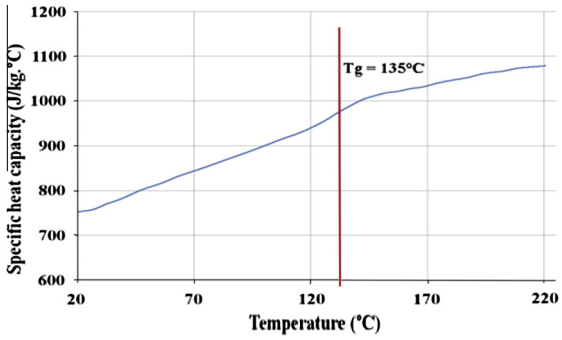

Fig. 13. Specific heat transfer of PC glass fiber.

5. Conclusion and prospects

The aim of this study was to determine thermo-physical and optical characterization of UD thermoplastic composites materials. Knowledge of these parameters is of utmost importance to better understanding of any process that involves laser processing of materials. These properties play an important role during the simulation of the welding process. The transmittivity coefficient (τ_λ) and reflectivity coefficient (ρ_λ) were determined using two approaches. A simplified experimental approach and numerical approach based on an inverse method program. The comparison showed a fair agreement between them. In another part of this study, a well-design device has been also developed in order to evaluate orthotropic thermal conductivities of composites. And finally we compared the experimental results to the analytical method concerning modeling thermal conductivities in composites. The comparison showed also a fair agreement between them, which gives confidence to use the developed model with acceptable accuracy. In future works (Part B), we will present a developed transient numerical model, based both on conduction and radiation mode heat transfer whose goal is to simulate infrared transmission welding process. The commercial FEM software COMSOL Multiphysics® will be used to obtain the temperature field by implementing a developed 3D heat source. And finally, the numerical results will be compared with experimental results in order to valid the heat transfer model.

Conflict of interest

Author has confirmed that there is no conflict of interest.

References

[1] A.C. Akué asséko, B. Cosson, F. Schmidt, Y. Le Maoult, E. Lafranche, Modelling and simulation of transmission laser welding process of thermoplastics composites, Esaform 2013. <www.scientific.net/KEM>.
[2] A.C. Akué asséko, B. Cosson, Schmidt F., Y. Le Maoult, E. Lafranche, Analytical and numerical modeling of light scattering in composite transmission laser welding process, Int.J. Mater. Form. (2013).
[3] A.C. Akué asséko, B. Cosson, F.Schmidt, Y. Le Maoult, R. Gilblas, E. Lafranche, Thermal modeling in composite transmission laser welding process: light scattering and absorption coupling, Esaform 2014. 1992, DOI 10.4028/<www.scientific.net/KEM.611-612.1560>.
[4] R. Siegel, J. Howell, Thermal Radiation Heat Transfer, third ed., Hemisphere Publishing Corporation, 1992.
[5] G.N. Labeas, G.A. Moraitis, C.V. Katsiropoulos, Optimization of laser transmission welding process for thermoplastic composite parts using thermo-mechanical simulation, J. Compos. Mater. 44 (1) (2010) 113–130.
[6] N.S. Shanmugam, G. Buvanashekaran, K. Sankaranarayanasamy, S. Ramesh Kumar, A transient finite element simulation of the temperature and bead profiles of T-joint laser welds, Mater. Des. 31 (9) (Oct. 2010) 4528–4542.
[7] D.A. Grewell, A. Benatar, Plastics and Composites: Welding Handbook, Hanser Verlag, 2003.
[8] J.M.P. Coelho, M.A. Abreu, F. Carvalho Rodrigues, Modelling the spot shape influence on high-speed transmission lap welding of thermoplastics films, Opt. Lasers Eng. 46 (1) (2008) 55–61.
[9] M. Ilie, J.-C. Kneip, S. Matteï, A. Nichici, C. Roze, T. Girasole, Through-transmission laser welding of polymers – temperature field modeling and infrared investigation, Infrared Phys. Technol. 51 (1) (2007) 73–79.
[10] M. Ilie, D. Grevey, S. Mattei, E. Cicala, V. Stoica, Diode laser welding of ABS: Experiments and process modeling, arXiv:1002.1241, Feb. 2010.
[11] Z.B. Hou, R. Komanduri, General solutions for stationary/moving plane heat source problems in manufacturing and tribology, Int. J. Heat Mass Transf. 43 (10) (2000) 1679–1698.
[12] K.J. Suthar, J. Patten, L. Dong, H. Abdel-Aal, Estimation of temperature distribution in silicon during micro laser assisted machining (2008) 301–309.
[13] M. Geiger, T. Frick, M. Schmidt, Optical properties of plastics and their role for the modelling of the laser transmission welding process, German Acad. Soc. Prod. Eng. 3 (2009) 49–55, http://dx.doi.org/10.1007/s11740-008-0141-1.
[14] B. Cosson, M. Deléglise, W. Knapp, Numerical analysis of thermoplastic composites laser welding using ray tracing method, Compos. B Eng. (2014), http://dx.doi.org/10.1016/j.compositesb.2014.08.028.
[15] M. Troughton, Chapter 13 – Laser Welding, in: Handbook of Plastics Joining, William Andrew Publishing, Norwich, NY, 1997, pp. 101–104.
[16] Monteix, Serge, Modélisation du chauffage convecto-radiatif de préformes en P.E.T. pour la mise en forme de corps creux, PhD thesis (in french), Institut Clément Ader (ICA-Albi), 2001.
[17] Bordival, Maxime, Modélisation et optimisation numérique de l'étape de chauffage infrarouge par fabrication de bouteilles en PET par injection-soufflage., PhD thesis (in french), Institut Clément Ader (ICA-Albi), 2009.
[18] J-L. Bailleul, D. Delaunay, Y. Jarny, T. Jurkowski, Thermal conductivity of unidirectional reinforced composite material. Experimental measurement as a function of state of cure, J. Reinf. Plast. Compos. (2001) 52–64.
[19] P.-E. Gill, W. Murray, M.-A. Saunders, User's guide for SNOPT version 7, Software for Large-Scale Nonlinear Programming (2008).
[20] Maxime Villière, Damien Lecointe, Vincent Sobotka, Nicolas Boyard, Didier Delaunay, Experimental determination and modeling of thermal conductivity tensor of carbon/epoxy composite, Composite Part A 46 (2013) 60–68.
[21] S. Nakouzi, Modélisation du procédé de cuisson de composites infusés par chauffage infra rouge, PhD thesis (in french), Institut Clément Ader (ICA-Albi), 2012.